Anal. Chem. **2010,** *82,* 9194–9200

Ultrasensitive Sensing of Hg^{2+} and CH_3Hg^+ Based on the Fluorescence Quenching of Lysozyme Type VI-Stabilized Gold Nanoclusters

Yen-Hsiu Lin[†] and Wei-Lung Tseng*[,†,‡]

Department of Chemistry, National Sun Yat-sen University, 70, Lien-hai Road, Kaohsiung, Taiwan 804, and National Sun Yat-sen University-Kaohsiung Medical University Joint Research Center, Kaohsiung, Taiwan

This study presents a one-step approach to prepare lysozyme type VI-stabilized gold nanoclusters (Lys VI-AuNCs) for the ultrasensitive detection of Hg^{2+} and CH_3Hg^+ based on fluorescence quenching. The optical properties and size of Lys VI-AuNCs are highly dependent on the concentration of Lys VI, which acts as both a reducing and a stabilizing agent. With an increase in the concentration of Lys VI, we observed a systematic blue shift in the fluorescence maxima, an increase in the quantum yields, and a reduction in the particle size. When using 25 mg/mL Lys VI as a reducing agent, the formed Lys VI-AuNCs (denoted as Au-631) were found to be highly stable in a high-concentration glutathione or NaCl. Additionally, the Au-631 were capable of sensing Hg^{2+} and CH_3Hg^+ through the interaction between Hg^{2+}/CH_3Hg^+ and Au^+ on the Au surface; the limits of detection (LODs) for Hg^{2+} and CH_3Hg^+ were 3 pM and 4 nM, respectively. The selectivity of this probe is more than 500-fold for Hg^{2+} over any metal ions. As compared to bovine serum albumin-stabilized AuNCs, Au-631 provided an approximately 330-fold improvement in the detection of Hg^{2+}. To the best of our knowledge, Au-631 not only provide the first example for detecting CH_3Hg^+ but also have the lowest LOD value for Hg^{2+} when compared to other AuNC-based Hg^{2+} sensors. Importantly, this probe was successfully applied to the determination of Hg^{2+} and CH_3Hg^+ in seawater.

The quantification of mercury in the aquatic environment and biological system is of considerable interest because it poses a severe risk to human health. One of the most stable inorganic forms of mercury, solvated mercuric ion (Hg^{2+}), can damage the brain, heart, kidney, stomach, and intestines, even at very low concentrations.[1] Microbial biomethylation of Hg^{2+} generates methylmercury (CH_3Hg^+), which bioaccumulates in the human body through the food chain, for example, in the tissue of fish.[2] Exposure to CH_3Hg^+ can adversely affect human neurodevelopment.[3] Methods currently available for detecting Hg^{2+} and CH_3Hg^+ include atomic absorption spectrometry, atomic fluorescence spectrometry, and inductively coupled plasma mass spectrometry.[4] These element-specific detectors are typically coupled with gas chromatography, high performance liquid chromatography, and capillary electrophoresis. However, these instrument techniques are rather complicated, time-consuming, and costly, as well as not being appropriate for point-of-use applications.

In response to these drawbacks, massive sensors have been developed for the simple and rapid tracking of Hg^{2+}, based on fluorophores,[5] chromophores,[5] T-rich DNA,[6] DNAzyme,[7] and semiconductor quantum dots.[8] Alternatively, gold nanoparticles (AuNPs) are promising materials for determining Hg^{2+} due to their convenient surface conjugation with molecular probes and remarkable plasmon-resonant optical properties. Because the surface plasmon resonance (SPR) band of the AuNPs is highly susceptible to the distance between each NP, the Hg^{2+}-induced aggregation of alkanethiol-capped AuNPs results in the formation of a new SPR band at longer wavelengths.[9−11] This aggregation is caused by the coordination between the carboxylic group of alkanethiol and Hg^{2+}. The Hg^{2+}-induced NP aggregation also amplifies the intensity of the hyper Rayleigh scattering.[11] Additionally, Hg^{2+} is capable of selectively coordinating thymine (T) bases. The melting temperature of the cDNA containing the T−Hg^{2+}−T complex is higher than that containing a T−T mismatch.[12] On the basis of this concept, DNA-

* To whom correspondence should be addressed. Fax: 011-886-7-3684046. E-mail: tsengwl@mail.nsysu.edu.tw.

† National Sun Yat-sen University.

‡ National Sun Yat-sen University-Kaohsiung Medical University Joint Research Center.

(1) Holmes, P.; James, K. A.; Levy, L. S. *Sci. Total Environ.* **2009**, *408*, 171–182.

(2) Merritt, K. A.; Amirbahman, A. *Earth-Sci. Rev.* **2009**, *96*, 54–66.

(3) Castoldi, A. F.; Johansson, C.; Onishchenko, N.; Coccini, T.; Roda, E.; Vahter, M.; Ceccatelli, S.; Manzo, L. *Regul. Toxicol. Pharmacol.* **2008**, *51*, 201–214.

(4) Leopold, K.; Foulkes, M.; Worsfold, P. *Anal. Chim. Acta* **2010**, *663*, 127–138.

(5) Nolan, E. M.; Lippard, S. J. *Chem. Rev.* **2008**, *108*, 3443–3480.

(6) Wang, J.; Liu, B. *Chem. Commun.* **2008**, 4759–4761.

(7) Hollenstein, M.; Hipolito, C.; Lam, C.; Dietrich, D.; Perrin, D. M. *Angew. Chem., Int. Ed.* **2008**, *47*, 4346–4350.

(8) Long, Y.; Jiang, D.; Zhu, X.; Wang, J.; Zhou, F. *Anal. Chem.* **2009**, *81*, 2652–2657.

(9) Huang, C.-C.; Chang, H.-T. *Chem. Commun.* **2007**, 1215–1217.

(10) Yu, C.-J.; Tseng, W.-L. *Langmuir* **2008**, *24*, 12717–12722.

(11) Darbha, G. K.; Singh, A. K.; Rai, U. S.; Yu, E.; Yu, H.; Chandra Ray, P. *J. Am. Chem. Soc.* **2008**, *130*, 8038–8043.

(12) Miyake, Y.; Togashi, H.; Tashiro, M.; Yamaguchi, H.; Oda, S.; Kudo, M.; Tanaka, Y.; Kondo, Y.; Sawa, R.; Fujimoto, T.; Machinami, T.; Ono, A. *J. Am. Chem. Soc.* **2006**, *128*, 2172–2173.

10.1021/ac101427y
Published on Web 10/18/2010

functionalized AuNPs selectively aggregate in the presence of Hg^{2+} based on T−Hg^{2+}−T coordination and temperature control.[13,14] On the other hand, a single strand of T-rich DNA enables citrate-capped AuNPs to be stabilized in a high-salt solution.[15−17] The presence of Hg^{2+} leads to a change in the conformation of the T-rich DNA, which has been removed from the NP surface. At the same time, salt-induced NP aggregation occurs. The sensitivity of this kind of sensor can be effectively improved by varying the number of T−T mismatches in the DNA duplexes[15] and adding Mn^{2+} to the sensing system.[17]

Recently, Au nanoclusters (AuNCs) have also been considered as Hg^{2+} sensors based on the quenching of their fluorescence.[18,19] In contrast to the other alkanethiol ligands, 11-mercaptoundecanoic acid-capped AuNCs exhibit relatively high quantum yields (QYs) and are capable of sensing Hg^{2+} via NP aggregation-induced fluorescence quenching.[18] Moreover, bovine serum albumin-stabilized AuNCs (BSA-AuNCs) have been demonstrated to be sensitive and selective to Hg^{2+} through the strong interaction of Hg^{2+} and Au^{+} on the Au surface.[19] Taking advantage of the high QY (∼6%) of BSA-AuNCs, the limit of detection (LOD) of Hg^{2+} at a signal-to-noise ratio of 3 was down to 0.5 nM. Although the above-mentioned sensors all provided high sensitivity and selectivity toward Hg^{2+}, they have not been yet utilized for sensing Hg^{2+} in complex matrix, such as seawater. Moreover, no study reported that CH_3Hg^{+} could be detected using AuNP- and AuNC-based sensors.

This study presents an ultrasensitive method for sensing Hg^{2+} and CH_3Hg^{+} based on the fluorescence quenching of lysozyme type VI-stabilized AuNCs (Lys VI-AuNCs), which is caused by the high affinity between Hg^{2+} and Au^{+} on the Au surface.[19] The roles of Lys VI in the synthesis of AuNCs are to act as a reducing agent and stabilizing ligand. When using 25 mg/mL Lys VI as a reducing agent, the formed Lys VI-AuNCs had more Au^{+} on the surface of Au core than BSA-AuNCs and thus exhibited a stronger interaction with Hg^{2+}. As a result, the as-prepared Lys VI-AuNCs were capable of detecting down to 10 pM (2.7 ppt) of Hg^{2+} and 15 nM (3.7 ppb) of CH_3Hg^{+}. To demonstrate the practicality of this probe, it is further applied to the determination of Hg^{2+} and CH_3Hg^{+} in seawater.

EXPERIMENTAL SECTION

Chemicals. Lys VI (chicken eggwhite) was ordered from MP Biomedicals (Irvine, CA). Lys (chicken eggwhite) and BSA (bovine plasma) were purchased from Sigma-Aldrich (St. Louis, MO). $HAuCl_4$, NaOH, LiCl, NaCl, KCl, $MgCl_2$, $CaCl_2$, $SrCl_2$, $BaCl_2$, $FeCl_2$, $FeCl_3$, $CoCl_2$, $NiCl_2$, $CuCl_2$, $ZnCl_2$, $MnCl_2$, AgCl, $Cd(ClO_4)_2$, $Pb(NO_3)_2$, $CrCl_3$, $HgCl_2$, NaB_4O_7, NaH_2PO_4, Na_2HPO_4, Na_3PO_4, H_3BO_3, CH_3COONa, $Na_3C_6H_5O_7$, $Na_2S_2O_3$, $NaHCO_3$, Na_2CO_3, Na_2SO_4, $Na_2S_2O_3$, $NaNO_3$, $NaNO_2$, $NaClO_4$, NaF, NaCl, NaBr, KI, and KIO_3 were obtained from Acros (Geel, Belgium). CH_3HgCl was ordered from TCI (Tokyo, Japan). Milli-Q ultrapure water (Milli-pore, Hamburg, Germany) was used in all of the experiments.

Synthesis of Protein-Modified AuNCs. The AuNCs were synthesized by chemical reduction of $HAuCl_4$ with Lys VI. A solution of Lys VI (5 mL, 10−40 mg/mL) was added to an equal volume of 10 mM $HAuCl_4$. The mixture was vigorously stirred for 2 min, followed by the rapid addition of NaOH (1 M, 5 μL). The resulting solution was incubated overnight at 37 °C. To investigate the effect of the type of protein on the fluorescence properties, we replaced Lys VI with Lys or BSA, one at a time.

Characterization of the AuNCs. The absorption and fluorescence spectra of the AuNCs were obtained using a double-beam UV−visible spectrophotometer (Cintra 10e; GBC, Victoria, Australia) and a Hitachi F-7000 fluorometer (Hitachi, Tokyo, Japan), respectively. The size and size distribution of the AuNCs were measured using dynamic light scattering (DLS; N5 submicrometer particle size analyzer, Beckman Coulter Inc., U.S.), respectively. The zeta potentials of the AuNCs were determined using Delsa nano zeta potential and submicrometer particle size analyzer (Beckman Coulter Inc., U.S.). Time-resolved fluorescence measurements were performed on an OB920 single-photon counting fluorometer (Edinburgh Analytical Instruments) with a pulsed nanosecond nitrogen lamp as excitation source. The elemental compositions of the Lys VI-AuNCs were measured by JAMP-9500F auger electron spectroscopy (JEOL, Japan). The molecular weight of the Lys VI-AuNCs was analyzed by mixing the cleaned Lys VI-AuNCs with equal volume of α-cyano-4-hydroxy cinnamic acid, and then using the Autoflex MALDI-TOF system (Bruker Daltonics, Germany) to measure the m/z value of the Lys VI-AuNCs.

Fluorescence Assay of Hg^{2+} and CH_3Hg^{+}. Hg^{2+} (2×10^{-11} to 2×10^{-5} M), CH_3Hg^{+} (3×10^{-8} to 1×10^{-5} M), other metal ions, and anions (10^{-4} M) were separately added to an equal volume of the Lys VI-AuNCs. After 0−30 min, the mixed solutions were transferred separately into a 1 mL quartz cuvette. Their fluorescence spectra were recorded by operating the fluorescence spectrophotometer at an excitation wavelength of 400 nm.

Seawater samples were collected from the ocean near our campus. A series of samples were prepared by "spiking" them with standard solutions of Hg^{2+} or CH_3Hg^{+}. The resulting solutions were added to an equal volume of the Lys VI-AuNCs. After 10 min, their fluorescence spectra were recorded at an excitation wavelength of 400 nm.

RESULTS AND DISCUSSION

Effect of the Concentration of Lys VI. Lys has been demonstrated to act as both a reducing and a stabilizing agent for producing various kinds of NPs, including AuNPs,[20] AgNPs,[21] zirconia particles,[22] silica NPs,[23] and titanic NPs.[23] Thus, the AuNCs via a reduction of $HAuCl_4$ were prepared with different

(13) Lee, J. S.; Han, M. S.; Mirkin, C. A. *Angew. Chem., Int. Ed.* **2007**, *46*, 4093–4096.
(14) Xue, X.; Wang, F.; Liu, X. *J. Am. Chem. Soc.* **2008**, *130*, 3244–3245.
(15) Xu, X.; Wang, J.; Jiao, K.; Yang, X. *Biosens. Bioelectron.* **2009**, *24*, 3153–3158.
(16) Li, D.; Wieckowska, A.; Willner, I. *Angew. Chem., Int. Ed.* **2008**, *47*, 3927–3931.
(17) Yu, C.-J.; Cheng, T.-L.; Tseng, W.-L. *Biosens. Bioelectron.* **2009**, *25*, 204–210.
(18) Huang, C.-C.; Yang, Z.; Lee, K.-H.; Chang, H.-T. *Angew. Chem., Int. Ed.* **2007**, *46*, 6824–6828.
(19) Xie, J.; Zheng, Y.; Ying, J. Y. *Chem. Commun.* **2010**, *46*, 961–963.
(20) Yang, T.; Li, Z.; Wang, L.; Guo, C.; Sun, Y. *Langmuir* **2007**, *23*, 10533–10538.
(21) Eby, D. M.; Schaeublin, N. M.; Farrington, K. E.; Hussain, S. M.; Johnson, G. R. *ACS Nano* **2009**, *3*, 984–994.
(22) Jiang, Y.; Yang, D.; Zhang, L.; Jiang, Y.; Zhang, Y.; Li, J.; Jiang, Z. *Ind. Eng. Chem. Res.* **2008**, *47*, 1876–1882.
(23) Luckarift, H. R.; Dickerson, M. B.; Sandhage, K. H.; Spain, J. C. *Small* **2006**, *2*, 640–643.

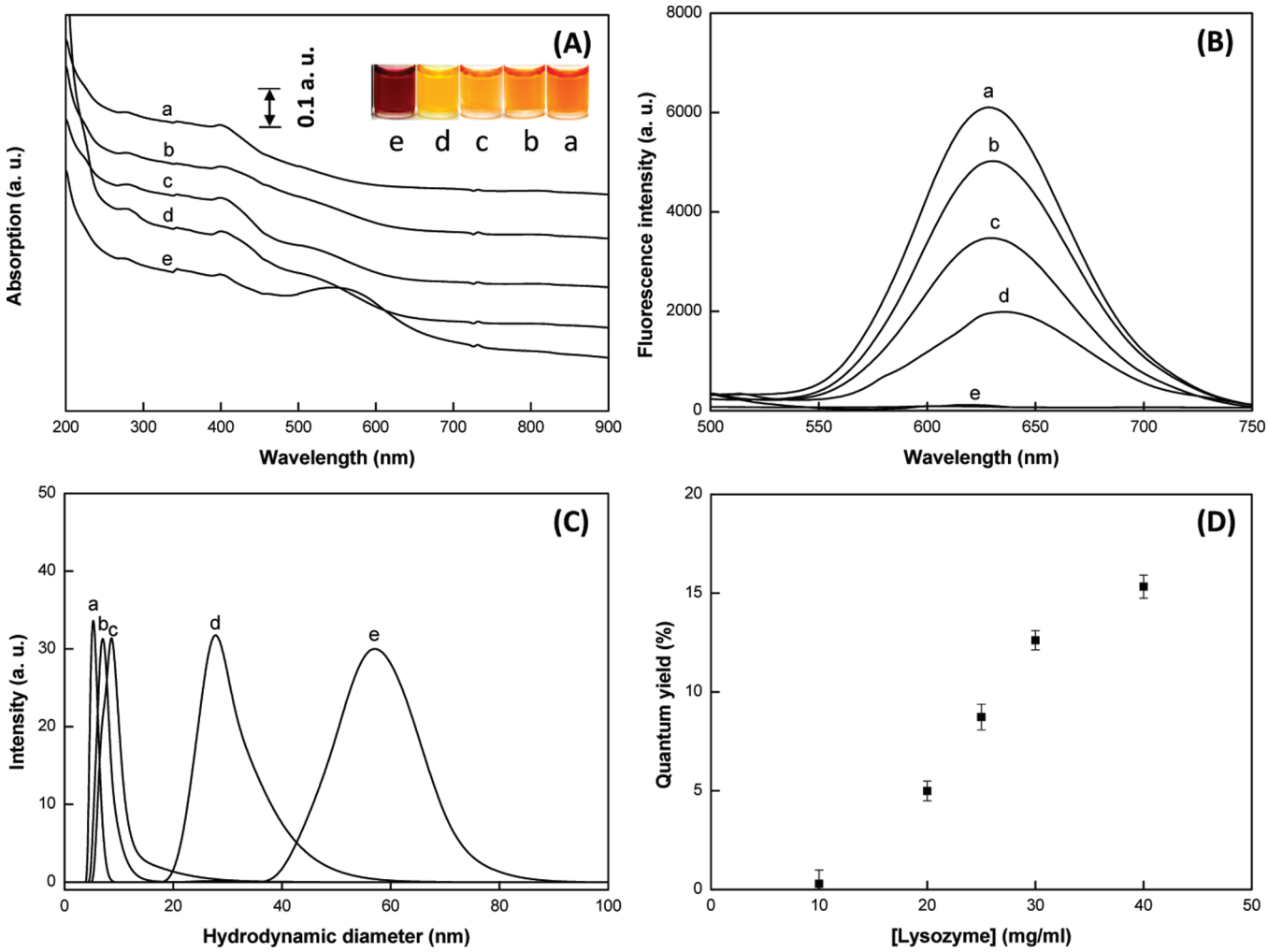

Figure 1. (A) Absorption spectra and photographs, (B) fluorescence spectra, (C) DLS spectra, and (D) QYs of the Lys VI-AuNCs. The Lys VI-AuNCs were prepared through reduction of $HAuCl_4$ with (a) 40, (b) 30, (c) 25, (d) 20, and (e) 10 mg/mL Lys VI. The excitation wavelength was set to 400 nm.

concentrations of Lys VI. It should be noted that the reduction ability of Lys VI was not activated until the reaction pH was adjusted to pH 12.0 with NaOH.[24] In the concentration range of 20−40 mg/mL Lys VI, the as-prepared particles exhibited absorption bands centered at a wavelength of 400 nm (curves a−d in Figure 1A) and a brown color (insets a−d in Figure 1A). The absorption spectral profiles of these particles resembled those of thiol-protected AuNCs[18,25,26] and polynuclear gold(I) complexes,[27,28] which all exhibited a broad absorption band centered within the wavelength range between 300 and 700 nm. On the basis of this literature and our observation, it is suggested that the absorption of Lys VI-AuNCs at 400 nm originated from metal-centered ($Au\ 5d^{10}$ to 6sp interband transitions) and/or ligand−metal charge-transfer transitions.[29−31] When the concentration of Lys VI was decreased to 10 mg/mL, the color of the as-prepared solution underwent a distinct change (inset e in Figure 1A). Two absorption bands were centered at wavelengths of 400 nm (AuNCs) and 547 nm (AuNPs), probably implying the formation of the AuNCs and AuNPs (curve e in Figure 1A). To support this hypothesis, the as-prepared solution was centrifuged to remove large-size AuNPs. The obtained supernatant displayed the characteristic color and absorption band of the AuNCs (Figure S1, Supporting Information).

As shown in Figure 1B, the fluorescence maxima of the AuNCs were shifted from 636 to 628 nm, while the concentrations of Lys VI were increased from 20 to 40 mg/mL. Moreover, an increase in the concentration of Lys VI led to the reduction of the size of the AuNCs (Figure 1C). The blue shift in the fluorescence maxima with a reduction of particle size is known in terms of an increase in the energy gap between the $5d^{10}$ band and the unoccupied states of the conduction (6sp) band levels.[26,28] This result also reflects the fact that Lys VI catalyzed the formation of the AuNCs by acting as the sole reducing agent. It is asserted that the role of Lys VI in the synthesis of the AuNCs is similar to that of citrate in the synthesis of AuNPs.[32] Besides, the fluorescence intensity and QYs of the AuNCs gradually decreased with the increasing

(24) Xie, J.; Zheng, Y.; Ying, J. Y. *J. Am. Chem. Soc.* **2009**, *131*, 888–889.
(25) Negishi, Y.; Tsukuda, T. *Chem. Phys. Lett.* **2004**, *383*, 161–165.
(26) Negishi, Y.; Nobusada, K.; Tsukuda, T. *J. Am. Chem. Soc.* **2005**, *127*, 5261–5270.
(27) Duan, H.; Nie, S. *J. Am. Chem. Soc.* **2007**, *129*, 2412–2413.
(28) Zheng, J.; Nicovich, P. R.; Dickson, R. M. *Annu. Rev. Phys. Chem.* **2007**, *58*, 409–431.
(29) Forward, J. M.; Bohmann, D.; Fackler, J. P.; Staples, R. J. *Inorg. Chem.* **1995**, *34*, 6330–6336.
(30) Vogler, A.; Kunkely, H. *Coord. Chem. Rev.* **2001**, *219*, 489–507.
(31) Yam, V. W. W.; Lo, K. K. W. *Chem. Soc. Rev.* **1999**, *28*, 323–334.

size of the AuNCs (Figure 1B and D). Because the surface-to-volume ratio increases with reducing the particle size, a larger fraction of the NC core atoms becomes involved in forming bonds with the core-capping ligands.[33−35] Thus, this phenomenon can probably be attributed to the effect of the surface ligand. Previous studies demonstrate that the fluorescence behavior of the AuNCs is highly dependent on the type of the surface ligand, because their size is smaller than 2 nm.[33−35] At a concentration of 10 mg/mL of Lys VI, no apparent fluorescence bands were found due to the collisional quenching between fluorescent AuNCs and large-size AuNPs (curve e in Figure 1B).[36] The supernatant corresponding to the AuNCs fluoresced after the centrifugation of the above prepared solution (Figure S2, Supporting Information). However, the fluorescence intensity of the AuNCs synthesized by 10 mg/mL Lys VI was quite weaker than that of the AuNCs synthesized by 20−40 mg/mL Lys VI. In other words, the synthesis of the AuNCs is successful only if the concentration of Lys VI is higher than 10 mg/mL. To reduce the cost of preparing the AuNCs, 25 mg/mL of Lys VI was selected for the subsequent study. Meanwhile, different concentrations of Lys (obtained from another manufacture) were used to prepare the AuNCs. However, the fluorescence intensity and QYs (0.1−10%) of the as-prepared AuNCs are smaller than those of the Lys VI-AuNCs (Figure S3, Supporting Information). This is probably because protein powders from different manufacturers may vary in their content of salt and small molecular contaminants.[37]

Optical Properties and Stability of Lys VI-AuNCs. We examined the properties of Lys VI-AuNCs after they were prepared via a reduction of $HAuCl_4$ with 25 mg/mL Lys VI. The fluorescence band of the as-prepared Lys VI-AuNCs (denoted as Au-631) was centered at 631 nm when they were excited at 400 nm. This large Stokes shifts can prevent spectral cross-talk, thereby enhancing the detection signal. MALDI-TOF mass spectrometry was utilized for determining the molecular weight of the Au-631. The difference in molecular weight between the Lys VI and Au-631 was approximately 5 kDa (Figure S4, Supporting Information). Shichibu et al. report that the core etching of Au_{25} clusters did not occur, even in the presence of an excess amount of glutathione,[38] mainly because Au_{25} clusters had the closed-shell geometric structure.[39] Thus, the stability of the Au-631 was also tested in the presence of 0.1−5 mM glutathione. Figure 2A shows that the fluorescence intensity of the Au-631 remained almost constant with the increase in the concentration of glutathione. This result reveals the Au-631 are extremely stable in a solution of glutathione.

The QY of the Au-631 was approximately 9%, determined by means of a comparison with BSA-AuNCs (QY = 6%).[24] This QY is higher than that of alkanethiol-protected AuNCs.[18,25,26] Although polyamidoamine dendrimers- and polyethylenimine-stabilized AuNCs exhibit high QY of over 10%,[27,28] they suffer from a long reaction time, the production of large AuNPs, and/or the use of a toxic inorganic reducing agent ($NaBH_4$). The time dependence of the fluorescence reveals that the Au-631 have two lifetime components, which are the general characteristics of the AuNCs.[18,27,40] By fitting them to a biexponential fluorescence decay, lifetimes t_1 and t_2 were obtained for Au-631 of 455 and 1891 ns, respectively. The short lifetime component is likely to originate from singlet transitions between filled d band and sp conduction bands of the AuNCs, while the long lifetime component may be due to a triplet−singlet intraband transition.[40,41]

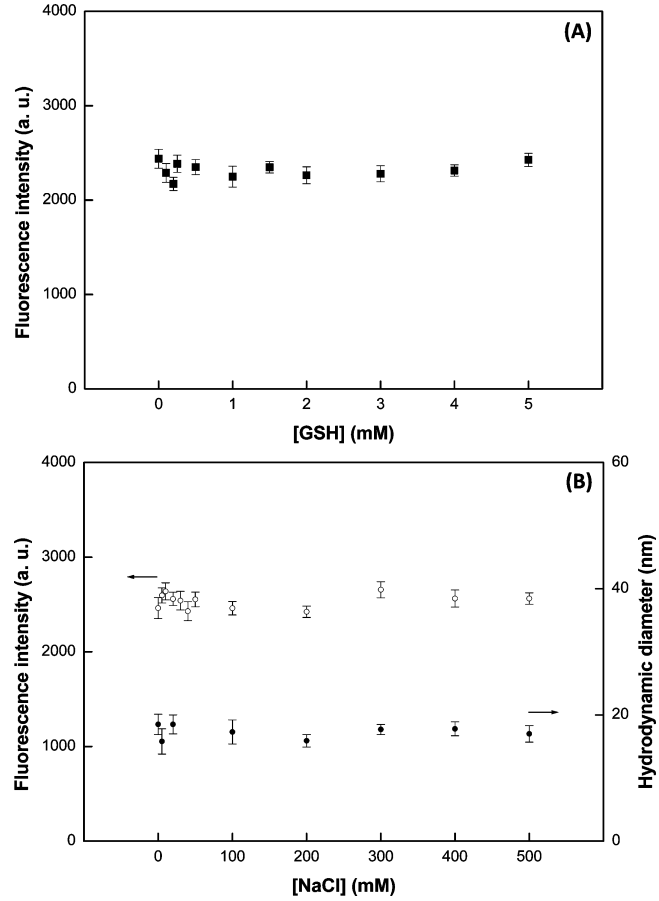

Figure 2. (A) Fluorescence intensities of the Au-631 in the presence of 0.1−5 mM glutathione. (B) Fluorescence intensities (○) and hydrodynamic sizes (●) of the Au-631 in a solution of 100 mM phosphate (pH 7.0) containing 5−500 mM NaCl. The excitation wavelength was set to 400 nm. The error bars represent standard deviations based on three independent measurements.

Next, the thickness of the Lys VI coating on the Au-631 was investigated. The average hydrodynamic diameter of the Au-631, determined by DLS measurements, was 8 ± 2 nm. The absorption band of the Au-631 centered at wavelengths of 400 nm indicated that their size was smaller than 3 nm. The difference in the hydrodynamic diameter between the Au-631 and a double width of Lys VI (4.5 × 3.0 × 3.0 nm, that is, length × width × height) was consistent with the size estimated by the absorption band of

(32) Ji, X. H.; Song, X. N.; Li, J.; Bai, Y. B.; Yang, W. S.; Peng, X. G. *J. Am. Chem. Soc.* **2007**, *129*, 13939–13948.
(33) Wang, G.; Guo, R.; Kalyuzhny, G.; Choi, J.-P.; Murray, R. W. *J. Phys. Chem. B* **2006**, *110*, 20282–20289.
(34) Wang, G.; Huang, T.; Murray, R. W.; Menard, L.; Nuzzo, R. G. *J. Am. Chem. Soc.* **2004**, *127*, 812–813.
(35) Liu, X.; Li, C.; Xu, J.; Lv, J.; Zhu, M.; Guo, Y.; Cui, S.; Liu, H.; Wang, S.; Li, Y. *J. Phys. Chem. C* **2008**, *112*, 10778–10783.
(36) Thomas, K. G.; Kamat, P. V. *Acc. Chem. Res.* **2003**, *36*, 888–898.
(37) Chayen, N. E.; Radcliffe, J. W.; Blow, D. M. *Protein Sci.* **1993**, *2*, 113–118.
(38) Shichibu, Y.; Negishi, Y.; Tsunoyama, H.; Kanehara, M.; Teranishi, T.; Tsukuda, T. *Small* **2007**, *3*, 835–839.
(39) Zhu, M.; Aikens, C. M.; Hollander, F. J.; Schatz, G. C.; Jin, R. *J. Am. Chem. Soc.* **2008**, *130*, 5883–5885.
(40) Link, S.; Beeby, A.; FitzGerald, S.; El-Sayed, M. A.; Schaaff, T. G.; Whetten, R. L. *J. Phys. Chem. B* **2002**, *106*, 3410–3415.
(41) Huang, T.; Murray, R. W. *J. Phys. Chem. B* **2001**, *105*, 12498–12502.

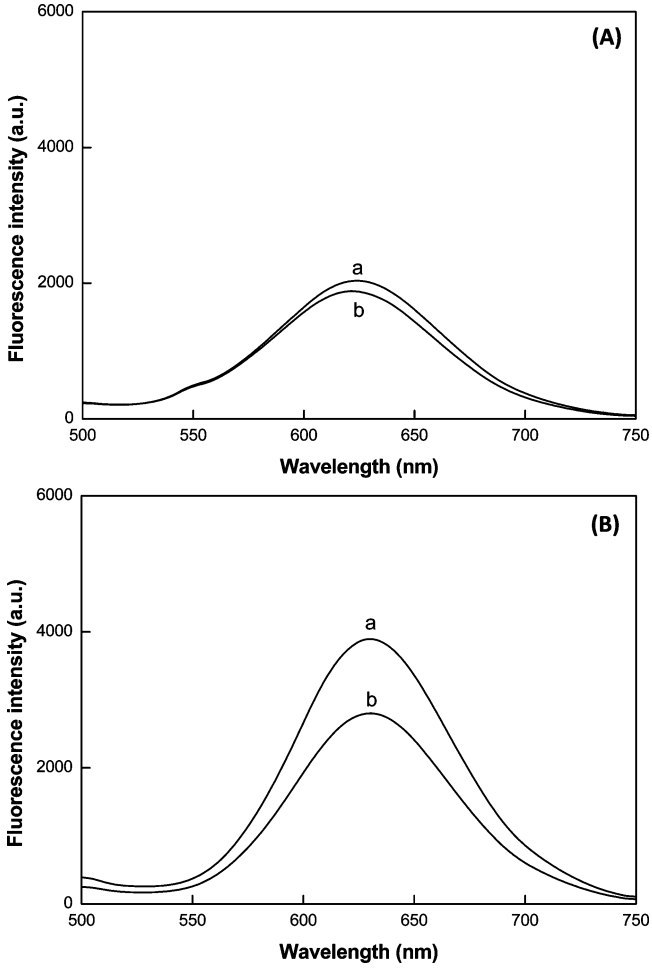

Figure 3. Fluorescence spectra of solutions of (A) BSA-AuNCs and (B) Au-631 (a) before and (b) after the addition of 0.1 μM Hg^{2+}. The excitation wavelength was set to 400 nm. The incubation time was 10 min.

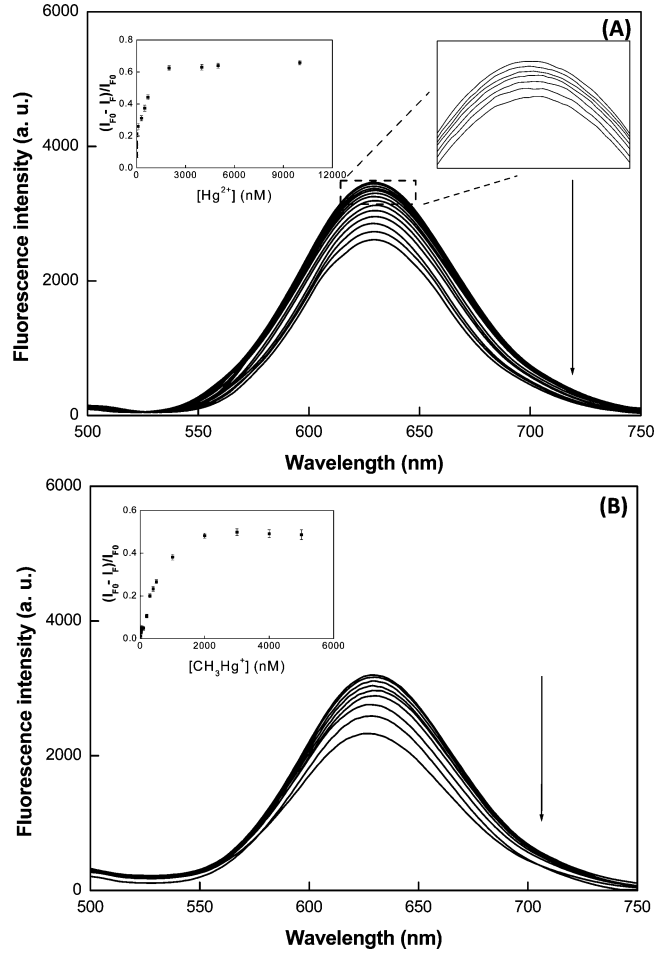

Figure 4. Fluorescence spectra of the Au-631 in the presence of increasing concentrations of (A) Hg^{2+} and (B) CH_3Hg^+. The arrows indicate the signal changes as increases in analyte concentrations (A, 0, 0.01, 0.05, 0.1, 1, 3, 5, 10, 100, 300, 500, 700, and 1200 nM; B, 0, 15, 20, 30, 40, 50, 200, 400, and 500 nM). Inset: Plots of the values of $(I_{F0} - I_F)/I_{F0}$ at 631 nm versus the concentrations of (A) Hg^{2+} and (B) CH_3Hg^+. The excitation wavelength was set to 400 nm. The incubation time was 10 min. The error bars represent standard deviations based on three independent measurements.

the Au-631, suggesting the formation of an Lys VI monolayer on the surfaces of the Au-631.[20] In comparison, larger BSA molecules ($4.0 \times 4.0 \times 14.0$ nm) could encapsulate the AuNCs when BSA was used to synthesize the AuNCs.[24] In addition, the stability of the Au-631 was evaluated by measuring the zeta potential. The zeta potential of the Au-631 was found to be 38 ± 2 mV, reflecting a great electrostatic repulsion between particles. The positive surface charges of the Au-631 revealed that the Lys VI molecules (pI = 11.3) were indeed attached to the Au surface. To confirm the stability of the Au-631, their fluorescence and hydrodynamic diameter were measured in a solution of 100 mM phosphate (pH 7.0) containing different concentrations of NaCl. As shown in Figure 2B, a slight change in the fluorescence intensity and hydrodynamic diameter revealed that Au-631 were stable under conditions of high ionic strength. This finding suggests that Au-631 have great potential for sensing molecules of interest under physiological conditions.

Ultrasensitive Sensing of Hg^{2+} and CH_3Hg^+. On the basis of previous studies,[19] the Hg^{2+}-induced fluorescence quenching of the BSA-AuNCs is probably attributed to the formation of metallophilic bonding between Hg^{2+} ($4f^{14}5d^{10}$) and Au^+ ($4f^{14}5d^{10}$). Therefore, it is important to measure the oxidation state of the Au-631 by XPS. The amount of Au^+ in Au-631 was calculated to be 41% by comparing the binding energy of Au (84.0 eV) with that of Au^+ (85.1 eV) (Figure S5, Supporting Information). In contrast, the BSA-AuNCs had a relatively small amount of Au^+ (~17%) on the surface of Au core.[24] This result may be because the reducing capability of the BSA containing 21 tyrosine residues is higher than that of the Lys VI containing 3 tyrosine residues. It should be noted that tyrosine can reduce Au(III) through its phenolic groups.[42] Because the Au-631 contained more Au^+ than the BSA-AuNCs, it is assumed that the Au-631 had higher affinity for Hg^{2+}, and thereby provided better sensitivity toward Hg^{2+}. To support this hypothesis, two kinds of AuNCs were compared in terms of the detection sensitivity of Hg^{2+}. When 0.1 μM Hg^{2+} was present in a solution of BSA-AuNCs, a slight decrease in the fluorescence was observed at 624 nm (Figure 3A). In contrast, adding the same concentration of Hg^{2+} to a solution of the Au-631 resulted in a remarkable decrease in fluorescence at 631 nm (Figure 3B). Obviously, Au-631 are more sensitive to Hg^{2+} than BSA-AuNCs. To test the sensitivity, a quantitative analysis of Hg^{2+} was

(42) Selvakannan, P. R.; Swami, A.; Srisathiyanarayanan, D.; Shirude, P. S.; Pasricha, R.; Mandale, A. B.; Sastry, M. *Langmuir* **2004**, *20*, 7825–7836.

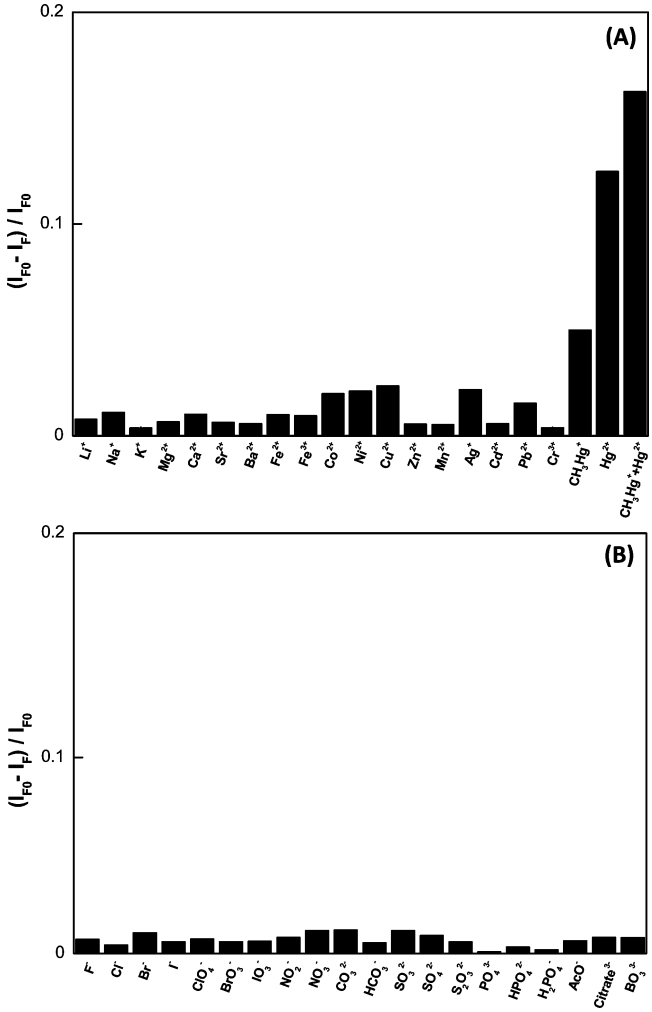

Figure 5. Relative fluorescence intensities $[(I_{F0} - I_F)/I_{F0}]$ at 631 nm of solutions of Au-631 after the addition of (A) Hg^{2+} (100 nM), CH_3Hg^+ (100 nM), and other metal ions (50 μM) and (B) anions (50 μM). The excitation wavelength was set to 400 nm. The incubation time was 10 min.

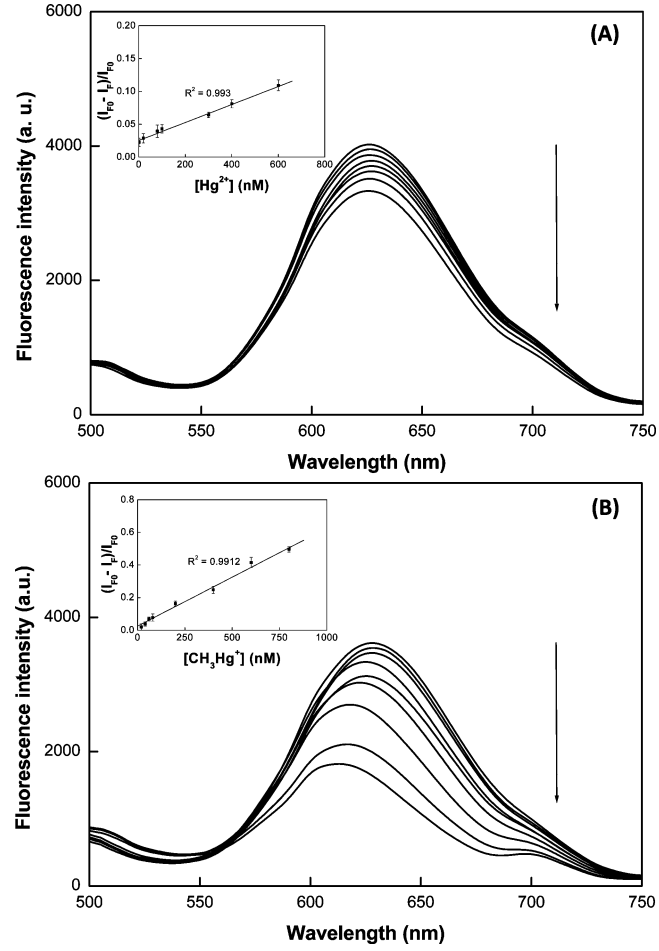

Figure 6. Fluorescent detection of (A) Hg^{2+} and (B) CH_3Hg^+ in seawater by the Au-631. Seawater samples were spiked with standard solutions of Hg^{2+} and CH_3Hg^+. The arrows indicate the signal changes as increases in analyte concentrations (A, 0, 1, 20, 80, 100, 300, 400, and 600 nM; B, 0, 20, 40, 60, 80, 200, 400, 600, and 800 nM). Inset: Plots of the values of $(I_{F0} - I_F)/I_{F0}$ at 631 nm versus the concentrations of (A) Hg^{2+} and (B) CH_3Hg^+. The excitation wavelength was set to 400 nm. The incubation time was 10 min. The error bars represent standard deviations based on three independent measurements.

performed using this probe of the Au-631. The optimal incubation time between the Au-631 and 0.1 μM Hg^{2+} was about 10 min (Figure S6, Supporting Information). The fluorescence spectra of the Au-631 displayed a gradual decrease in fluorescence at 631 nm with increasing Hg^{2+} concentration (Figure 4A). Plotting the value of $(I_{F0} - I_F)/I_{F0}$ versus the concentrations of Hg^{2+} gave two calibration curves (inset in Figure 4A). It should be noted that I_{F0} and I_F are the fluorescence intensities of the Au-631 before and after adding analytes, respectively. The correlation coefficients (R^2) were 0.9954 and 0.9949 for determining Hg^{2+} over the concentration ranges of 10−5000 pM and 10−1200 nM, respectively. The LOD at an S/N ratio of 3 for Hg^{2+} was 3 pM, which is much lower than the maximum level (10 nM, 2 ppb) of mercury in drinking water permitted by the United States Environmental Protection Agency. As compared to 11-mercaptoundecanoic acid-capped AuNCs,[18] BSA-AuNCs,[19] and Lys-AuNCs,[43] the Au-631 provide a 160−3300-fold improvement in sensitivity for the fluorescent detection of Hg^{2+} (Table S1, Supporting Information). Because the Hg^{2+}−Au^+ interaction induced the fluorescence quenching of the Au-631, it is assumed that Au-631 have such effect on CH_3Hg^+. Figure 4B shows that the fluorescence at 631 nm of the Au-631 gradually decreased when the concentrations of CH_3Hg^+ were increased from 15 to 2000 nM. The linear relationship of the value of $(I_{F0} - I_F)/I_{F0}$ versus CH_3Hg^+ concentration, as shown in the inset of Figure 4B, was from 15 to 500 nM ($R^2 = 0.9904$). The LOD of CH_3Hg^+ was estimated to be 4 nM.

The selectivity of the Au-631 toward Hg^{2+} and CH_3Hg^+ was tested next, and Figure 5A shows that changes in the relative fluorescence $[(I_{F0} - I_F)/I_{F0}]$ of the Au-631 occurred within 10 min after separately adding Hg^{2+} (100 nM), CH_3Hg^+ (100 nM), and other metal ions (50 μM). Addition of Hg^{2+}, CH_3Hg^+, or both to a solution of Au-631 caused a significant change in the value of $(I_{F0} - I_F)/I_{F0}$, whereas the remaining metal ions demonstrated a negligible effect in identical conditions. Moreover, Figure 5B displays a rare change in the value of $(I_{F0} - I_F)/I_{F0}$ after adding anions (50 μM) to a solution of Au-631. It

(43) Wei, H.; Wang, Z.; Yang, L.; Tian, S.; Hou, C.; Lu, Y. *Analyst* **2010**, *135*, 1406–1410.

is suggested that the selectivity of the Au-631 is more than 500-fold for Hg^{2+} and CH_3Hg^+ over any of the metal ions and anions. Additionally, we utilized DLS to prove that the sensing mechanism was based on the high-affinity metallophilic $Hg^{2+}-Au^+$ interaction, rather than the aggregation of the Au-631. As compared to the absence of Hg^{2+} and CH_3Hg^+, the average hydrodynamic diameter of the Au-631 remained almost constant after the addition of 100 nM Hg^{2+} and CH_3Hg^+ (Figure S7, Supporting Information). Thus, we ruled out the possibility that the Hg^{2+}- and CH_3Hg^+-induced aggregation of the Au-631 caused the fluorescence quenching.

The feasibility of the Au-631 for detecting Hg^{2+} and CH_3Hg^+ in seawater is, therefore, validated. An apparent decrease in fluorescence at 631 nm was observed after samples of seawater were spiked with standard solutions containing different concentrations of Hg^{2+} (Figure 6A). A similar result was reached in the measurement of CH_3Hg^+ (Figure 6B). The calibration curves for determining Hg^{2+} and CH_3Hg^+ in seawater were obtained by plotting the values of $(I_{F0} - I_F)/I_{F0}$ versus the concentrations of Hg^{2+} and CH_3Hg^+ over the range from 1 to 600 nM and from 20 to 800 nM, respectively (inset in Figure 6A and B). The LODs of Hg^{2+} (0.51 nM) and CH_3Hg^+ (5.90 nM) in seawater were higher than those in deionized water, probably because of the formation of $HgCl_2$ and CH_3HgCl complexes. These results suggest that Au-631 are applicable for determining Hg^{2+} and CH_3Hg^+ in environmental and biological samples.

CONCLUSION

We have presented a straightforward one-pot approach to synthesize high fluorescent AuNCs using Lys VI as both a reducing and a stabilizing agent. An increase in the concentration of Lys VI in a precursor solution resulted in an increase in QYs of the AuNCs and a reduction in particle size. After the reduction of $HAuCl_4$ by 25 mg/mL Lys VI, the formed Au-631 provided a number of distinctive advantages. First, the fluorescence intensity of the Au-631 remained almost constant in a high concentration of glutathione and a high-salinity solution. Second, to the best of our knowledge, this is the first example of the use of Au-based nanomaterials to detect CH_3Hg^+. Third, this approach provided excellent selectivity and the lowest LOD value for Hg^{2+} when compared to other AuNP- and AuNC-based sensors. Last, the Au-631 can be applied to detect Hg^{2+} and CH_3Hg^+ in a complex environment. Interestingly, it was found that Au-631 can discriminate Hg^{2+} and CH_3Hg^+ using ethylenediaminetetraacetic acid as a masking agent. This is a subject for further investigation.

ACKNOWLEDGMENT

We would like to thank the National Science Council (NSC 98-2113-M-110-009-MY3) and National Sun Yat-sen University-Kaohsiung Medical University Joint Research Center for financial support of this study. We also thank National Sun Yat-sen University and Center for Nanoscience & Nanotechnology for measurement of the fluorescence spectrum.

SUPPORTING INFORMATION AVAILABLE

Additional information as noted in text. This material is available free of charge via the Internet at http://pubs.acs.org.

Received for review June 1, 2010. Accepted October 4, 2010.

AC101427Y